Soft Matter

Colloidal stability dictates drop breakup under electric fields

Journal:	*Soft Matter*
Manuscript ID	SM-ART-07-2018-001545.R1
Article Type:	Paper
Date Submitted by the Author:	21-Sep-2018
Complete List of Authors:	Lanauze, Javier; Carnegie Mellon University, Department of Chemical Engineering Sengupta, Rajarshi; Carnegie Mellon University, Chemical Engineering Bleier, Blake; Carnegie Mellon University, Chemical Engineering Yezer, Benjamin; Carnegie Mellon University, Department of Chemical Engineering Khair, Aditya; Carnegie Mellon, Chemical Engineering Walker, Lynn; Carnegie Mellon University, Department of Chemical Engineering

Soft Matter

ARTICLE TYPE

Cite this: DOI: 10.1039/xxxxxxxxxx

Colloidal stability dictates drop breakup under electric fields†

Javier A. Lanauze,[a‡] Rajarshi Sengupta,[a‡] Blake J. Bleier,[a] Benjamin A. Yezer,[a] Aditya S. Khair[a] and Lynn M. Walker*[a]

Received Date
Accepted Date

DOI: 10.1039/xxxxxxxxxx

www.rsc.org/journalname

Electric fields can deform drops of fluid from their equilibrium shape, and induce breakup at sufficiently large field strengths. In this work, the electric field induced breakup of a squalane drop containing a colloidal suspension of carbon black particles with polyisobutylene succinimide (OLOA 11000) surfactant is studied. The drop is suspended in silicone oil. The breakup mode of a drop containing carbon black depends strongly on the suspension stability. It is observed that a drop of a stable suspension of carbon black has the same breakup mode as a drop with surfactant alone, i.e., without added carbon black. At lower electric fields, these drops break by the formation of lobes at the two ends of the drop; and at higher fields the homogeneous lobes break in a non-axisymmetric manner. However, a drop of an unstable suspension shows a drastically different breakup mode, and undergoes breakup much faster compared to a drop with surfactant alone. These drops elongate and form asymmetric lobes that develop into fingers and eventually disintegrate in an inhomogeneous, three-dimensional fashion. As a basis for comparison, the breakup of a pure squalane drop, and a squalane drop with equivalent surfactant concentrations but no carbon black particles is examined. Axisymmetric boundary integral computations are used to elucidate the mechanism of breakup. Our work demonstrates the impact of colloidal stability on the breakup of drops under an electric field. Colloidal instability on the time scale of drop deformation leads to rich and unexplored breakup phenomena.

1 Introduction

Liquid drops are subjected to electric fields in various industrial and scientific applications including inkjet printing[1–3], electroemulsification[4–6], electrospray mass spectrometry[7,8], printing of enzymes and proteins[9], structuring colloidal particles at fluid-fluid interfaces[10–12], and formation of Janus particles and capsules[13]. When an electric field is applied across a drop of fluid suspended in another fluid, electric stresses are generated at the interface, which deform the drop from its equilibrium shape. For perfectly conducting or perfectly dielectric drops suspended in a perfectly dielectric medium, the electric traction solely acts normal to the interface, and there is no fluid motion if the drop attains a steady deformed shape[14]. If both the drop and the suspending fluid are weakly conducting the electric traction has a tangential component in addition to the normal component, which drives an *electrohydrodynamic* fluid flow in both phases even when the drop reaches a steady deformed shape[15]. For these systems, the drop can deform either along the electric field into prolate shapes, or perpendicular to the direction of the applied field into oblate shapes[15]. Here we consider the prolate deformation of a weakly conducting drop suspended in a weakly conducting fluid.

Under sufficiently large field strengths, the drop undergoes breakup into smaller drops[14,16]. In all applications involving electric field manipulation of fluid-fluid systems, the mode of breakup needs to be understood. There have been a number of computational[17–25] and experimental[23,26–29] studies on drop deformation and breakup under electric fields. These studies broadly classify drop breakup into two modes. The first mode, called end pinching, is characterized by the elongation of the drop into a cylindrical thread, which develops bulbs at the two ends. This is followed by a detachment of the bulbs from the thread, resulting in drops having a size similar to the original drop. In the second mode, called tip-streaming, the drop develops conical ends from which drops having size two or three orders of magnitude smaller than the original drop are ejected. The resulting distribution of drop sizes is very different for these two breakup modes. Surfactant molecules in the system can change the breakup mode from

[a] *Department of Chemical Engineering, Carnegie Mellon University, Pittsburgh, PA 15213, USA. E-mail: lwalker@andrew.cmu.edu*

† Electronic Supplementary Information (ESI) available: Boundary integral computations with insoluble surfactant, eight supplementary movies. See DOI: 10.1039/cXsm00000x/

‡ These authors contributed equally to this work.

end pinching to tip-streaming for a certain window of surfactant concentration. At concentrations below and above this window the drop undergoes breakup by end pinching; for intermediate concentrations, tip-streaming is the observed breakup mode[30]. In systems where the surfactant concentration is high enough to drastically reduce the interfacial tension to $\leq 0.5 mN/m$, drops have been reported to undergo another transition from end pinching to a sudden catastrophic breakup into a fine mist of very small drops on time scales much smaller than tip-streaming or end pinching[31]. Such a mode of breakup is undesirable in applications like inkjet printing because it compromises the quality of the print, but could be advantageous in processes like emulsification, where the goal is to make smaller drops. Furthermore, in certain practical applications, like inkjet printing, the liquid drops subjected to electric fields contain colloidal dispersions stabilized with surfactant[3,32]. However, the breakup of a suspension loaded drop under an electric field has received little attention. In fact, homogeneity of the dispersed phase has not been considered in electric field driven breakup of drops.

In this work, we address this knowledge gap by quantifying the breakup mode of an oil drop containing fixed amount of carbon black particles under a uniform DC electric field. This system is chosen because carbon black suspensions of different degrees of stability can be formulated by varying the amount of surfactant (dispersant) present in the drop phase. First, the breakup of a squalane drop in the absence of surfactant and carbon black particles is characterized. Then, the breakup of a drop of a stable suspension, and a drop of an unstable suspension is studied. As a basis for comparison, drops having equivalent surfactant concentrations but no carbon black particles are also examined for breakup. A central conclusion of our work is that drops having differing suspension stability undergo radically different breakup modes. A drop of a stable suspension has the same breakup mode as a drop having an equivalent concentration of surfactant, but no particles. A drop of an unstable suspension undergoes an inhomogeneous breakup, which is drastically different from a drop having an equivalent surfactant concentration without particles. Boundary integral computations predict the experimentally observed homogeneous breakup modes, elucidating the mechanism of breakup.

2 Materials and Methods

2.1 Sample preparation and experimental setup

Samples of carbon black (Monarch 280, Cabot Corporation) and polyisobutylene succinimide surfactant (OLOA 11000, Chevron Oronite) suspended in squalane (Alfa Aesar) were produced in 50 ml vials at various concentrations of OLOA. The carbon black was reported to have a primary particle diameter of 30 nm. A primary particle aggregate diameter of 200 nm was determined from light scattering measurements (Zetasizer Nano ZS90). Reported surfactant concentrations are based on material as received, which is reported to be 75% surfactant and 25% mineral oil. We report the amount of added surfactant in parts OLOA per 100 parts carbon black (pph). Carbon black was baked under vacuum at 200°C for 4 hours and allowed to cool to remove trace amounts of water. Then, the particles were introduced into premixed samples of squalane and OLOA surfactant; the particle concentration was fixed at 3.3 g/L, equivalent to a carbon black volume fraction of 0.19%. The samples were sonicated (Cole-Parmer 750-Watt Ultrasonic Homogenizer) for 20 minutes and stored in a desiccator. Before each experiment, the samples were sonicated again for 30 minutes. The stability of carbon black in non-polar solvents is controlled by the amount of added surfactant[33–35]. At low surfactant concentrations the suspension is sterically stabilized; the carbon black particles aggregate and sediment over a timescale of minutes , yielding a clear supernatent. Above a critical surfactant concentration, the suspension is electrostatically stabilized, and the particles remain dispersed in solution over a timescale of, at least, months.[35]

The drop deformation experiments were performed in a cell whose schematic is shown in figure 1. A particle-loaded squalane drop was injected into a silicone oil medium from a 25 μL glass syringe with a 22 gauge needle. A voltage on the order of kV/cm was applied across two 5 cm $\times$ 5 cm brass electrodes separated at a distance of 2 cm using a high voltage DC power supply (Gamma High Voltage Research, Inc.). As soon as the electric field was applied, the time-dependent drop shape was recorded at a rate of 7.5 frames per second using a firewire camera (Guppy PRO F-125B, Allied Vision Technologies). Image analysis was conducted using ImageJ software. The material properties of the systems examined in this study are listed in table 1. The permittivity and resistivity of each fluid was measured via Electrochemical Impedance Spectroscopy[36]. The viscosity of each phase was extracted from the literature. Finally, the interfacial tension was acquired by fitting our previously developed linear theory, which quantifies the electric field induced transient deformation of a low conductivity drop[37], to the experimental timespan during which the drop deformation is small. Here, the deformation is quantified as the difference between the drop semi-axes parallel and normal to the applied field divided by the sum of the two. Although this theory does not account for surfactant, we use it to estimate the interfacial tension in the presence of OLOA, and OLOA and carbon black particles.

2.2 Computation of transient drop shape

We implement the boundary integral method to compute the electric field and fluid flow at the drop surface, as well as the resulting drop deformation. The differential governing equations are those described by Taylor's leaky dielectric model[15,38,39]. This model attributes the low conductivity of the fluids to the presence of a small concentration of charge carriers, which are transported to the interface by electric fields, giving rise to a surface charge density, q. The form and numerical solution procedure of the equations is discussed in Supplementary Information 1 (ESI†), and an overview is presented here. The procedure to evaluate the transient drop shapes is to sequentially solve for the electric field inside and outside the drop, and fluid flow inside and outside the drop, with interface conditions accounting for stress balance and charge conservation.

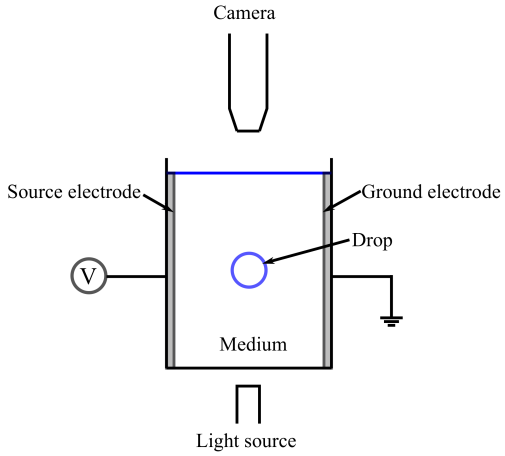

Fig. 1 Schematic of the experimental set-up used to perform drop deformation experiments. The two electrodes are placed $2\,cm$ apart, and have a square cross-section ($5\,cm \times 5\,cm$).

When surfactant molecules are present in the system, they are transported by the induced flow. This results in a non-uniform distribution of surfactant at the interface, which in turn drives a Marangoni flow, in conjunction with the electrohydrodynamic flow. To compare the breakup of a squalane drop with the OLOA surfactant, we incorporate insoluble surfactant in the boundary integral code by solving the interfacial surfactant transport equation[40] as an additional interface condition. Although OLOA is soluble in squalane, we neglect the kinetic exchange of OLOA from the interface to the bulk, and model it as an insoluble surfactant at the squalane-silicone oil interface.

Our computations are implemented to predict the qualitative transient drop shape achieved under certain experimental conditions. The computations assume a homogeneous drop phase and an axisymmetric drop shape during the deformation and breakup processes.

2.3 Material parameters and dimensionless groups

The drop deformation is quantified by the ratio of the permittivity $S = \varepsilon_i/\varepsilon_o$, resistivity $R = \chi_i/\chi_o$, and viscosity $M = \mu_i/\mu_o$ of the drop phase fluid to the medium phase fluid, the electric capillary number Ca , the electric Reynolds number Re and the Saville number Sa[38,39]. The subscripts denote the drop (inner, i) and medium (outer, o) phases, respectively. The electric capillary number, $Ca = \varepsilon_o E_\infty^2 a/\gamma$, is the ratio of the electrical stress ($\varepsilon_o E_\infty^2$) that deforms the drop, relative to the capillary stress (γ/a) that acts to restore the drop back to equilibrium. Here, E_∞ is the magnitude of the uniform applied field, a denotes the radius of a spherical drop, and γ represents the interfacial tension. The Saville number $Sa = \tau_e/\tau_c$, represents the ratio of the charging timescale $\tau_e = \varepsilon_o\chi_o$ to the capillary timescale $\tau_c = \mu_o a/\gamma$, and the electric Reynolds number $Re = \tau_e/\tau_f$, represents a ratio of the charging timescale to the flow timescale $\tau_f = a/U$, where the velocity scale, $U = \varepsilon_o a E_\infty^2/\mu_o$, is obtained from a balance between the viscous stresses and the electric stresses. In the presence on an insoluble surfactant, the deformation of the drop depends on an additional dimensionless group, the surface Peclet number, $Pe_s = \dfrac{a^2\varepsilon_o E_\infty^2}{D_s\mu_o}$, which denotes the rate of surfactant transport by convection to diffusion along the interface, D_s being the surface diffusion coefficient.

The material properties for the systems examined in this study are listed in table 1; the relevant dimensionless groups for all systems are listed in tables 2 and 3.

3 Results

3.1 Breakup of a squalane drop

We first examine the field induced breakup of a pure squalane drop suspended in silicone oil via experiment and computation. Here, the drop is more conductive ($R < 1$) and less viscous ($M < 1$) than the medium. The resulting transient drop deformation for this system (and all systems that follow) is along the electric field, i.e., the drop undergoes a prolate deformation. The applied field is 7.6 kV/cm, which is chosen as it is approximately the critical field strength required to induce the breakup of the pure squalane drop in our experiment.

The transient drop shape for this system is displayed in figure 2. In this figure (and all figures that follow), the applied electric field is directed from left to right. The change in the shape of the drop is quantified through changes in the dimensionless drop major semi-axis L/a. Here, L represents the half of the length of the drop parallel to the applied field; it is initially equal to the spherical drop radius a. The open circles denote the experimental measurement, and the solid curve denotes results from axisymmetric boundary integral computations conducted at the conditions of the experiment. The experiment shows that the squalane drop forms pointed ends and achieves breakup via tip-streaming at the end nearest to the left electrode. The measurement is illustrated until this point in time, $t = 14.1$ s. The inset at the top-left in figure 2 shows the experimentally observed drop shape at this point in time, and the eventual breakup through tip-streaming from both pointed ends of the drop at $t = 21.5$ s. The computationally predicted drop shapes at the same instants of time are also depicted as insets.

The computational curve is illustrated until $t = 14.1$ s for comparison against the experimental measurement; the inset at the bottom-right shows the full transient deformation of the drop, as predicted by the computation. The final deformation obtained from the computation is greater than the experimentally observed deformation before breakup. The computation predicts that the drop undergoes breakup by tip-streaming at $t = 52.3\,s$, while the experiment indicates that the drop undergoes breakup at $t = 21.5\,s$. Thus, although the there is a quantitative difference between the computations and experiments, the computations qualitatively capture the experimentally observed breakup mode.

3.2 Breakup of a drop containing a stable colloidal suspension

Next, we probe the electric field induced breakup of a drop containing a stable suspension of carbon black particles (Supplementary movie 1, ESI[†]). Here, the amount of added surfactant

Table 1 Material properties of a squalane drop suspended in silicone oil. Here, ε_r denotes the relative permittivity and "CB" denotes carbon black.

Phase	ε_r	$1/\chi$ (S/m)	μ (Pa s)	a (mm)	γ (mN/m)
medium–silicone oil	2.8	2.0×10^{-12}	4.80	–	–
drop–squalane (pure)	2.1	2.1×10^{-12}	0.03	0.6	4.6
drop–squalane (30 pph surfactant–no CB)	2.1	2.2×10^{-10}	0.03	0.7	5.2
drop–squalane (30 pph surfactant–with CB)	2.1	2.6×10^{-10}	0.03	0.6	1.4
drop–squalane (2 pph surfactant–no CB)	2.1	1.6×10^{-11}	0.03	0.6	–
drop–squalane (2 pph surfactant–with CB)	2.1	–	0.03	0.6	1.5

Table 2 Dimensionless groups that describe a squalane drop suspended in silicone oil. Here, "CB" denotes carbon black. For the pure squalane system, the applied field $E_\infty = 7.6$ kV/cm, while the remaining systems correspond to a field $E_\infty = 2.5$ kV/cm. Note that the electric capillary number Ca, the Saville number Sa, the electric Reynolds number Re, and the surface Peclet number Pe_s are all based on the medium properties.

System	Ca	Sa	Re	Pe_s	S	M	R
pure squalane	1.9	19.6	37.2	–	0.75	0.01	0.97
squalane (30 pph surfactant–no CB)	0.2	19.0	3.8	230	0.75	0.01	0.01
squalane (30 pph surfactant–with CB)	0.7	6.0	4.2	230	0.75	0.01	0.01
squalane (2 pph surfactant–no CB)	–	–	45.0	230	0.75	0.01	0.125
squalane (2 pph surfactant–with CB)	0.6	–	–	230	0.75	0.01	–

Table 3 Dimensionless groups that describe a squalane drop suspended in silicone oil. Here, "CB" denotes carbon black. The applied field $E_\infty = 5.3$ kV/cm. Note that the electric capillary number Ca, the Saville number Sa, the electric Reynolds number Re, and the surface Peclet number Pe_s are all based on the medium properties.

System	Ca	Sa	Re	Pe_s	S	M	R
squalane (30 pph surfactant–no CB)	0.9	19.0	17.1	1045	0.75	0.01	0.01
squalane (30 pph surfactant–with CB)	3.0	6.0	18.0	1045	0.75	0.01	0.01
squalane (2 pph surfactant–no CB)	–	–	202.0	1045	0.75	0.01	0.125
squalane (2 pph surfactant–with CB)	2.8	–	–	1045	0.75	0.01	–

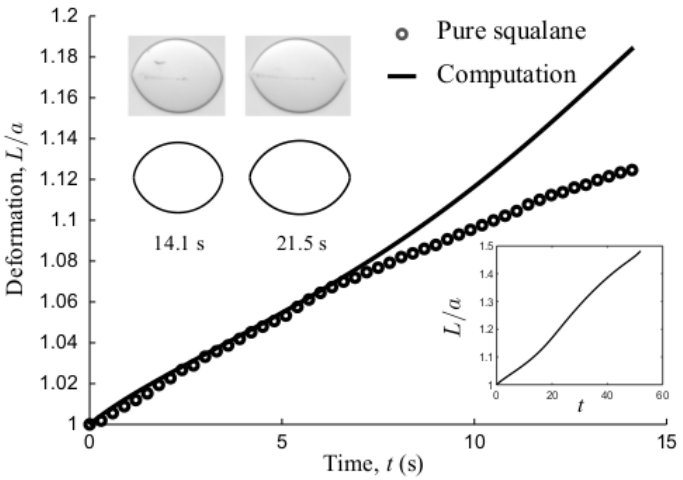

Fig. 2 Experiment and computation illustrating the transient deformation of a pure squalane drop suspended in silicone oil at an electric field strength $E_\infty = 7.6$ kV/cm. The material properties for this system are listed in table 1, while the relevant dimensionless groups are listed in table 2.

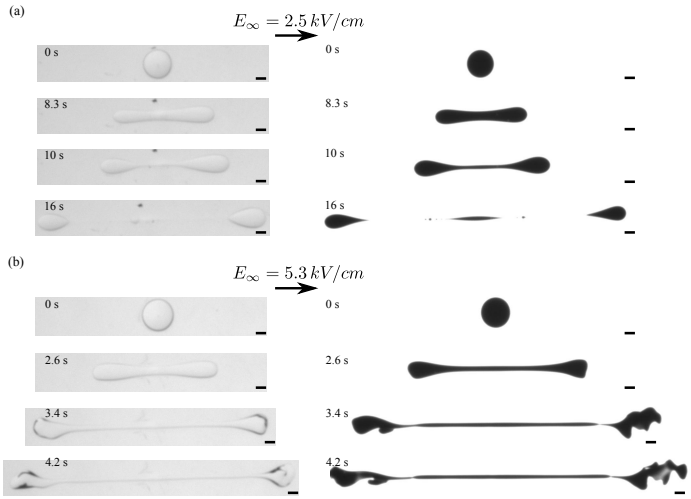

Fig. 3 Transient shapes of a drop of squalane with 0.12 wt% OLOA surfactant (left panel), and a drop of squalane with 3.3 g/L carbon black and 30 pph OLOA surfactant (right panel), subjected to an electric field of (*a*) 2.5 kV/cm, and (*b*) 5.3 kV/cm. Here, the drops are suspended in silicone oil. Scale bar: 0.5 mm.

(30 pph OLOA) is enough to provide stabilization of the suspension through electrostatic repulsion between the particles[33–35]. For this system, the carbon black particles remain dispersed throughout the suspending fluid over a timescale of at least months, which is much longer than the timescale of the experiment. As a basis for comparison, we examine the breakup of a drop containing an equivalent amount of total surfactant with no carbon black particles, which corresponds to 0.12 wt% OLOA (Supplementary movie 2, ESI†). This system undergoes breakup at an applied field of $E_\infty = 2.5$ kV/cm, which is three times lower than the electric field required to achieve the breakup of a pure squalane drop ($E_\infty = 7.6$ kV/cm). The two material properties that change on addition of surfactant and particles are the drop conductivity and interfacial tension. The reduced interfacial tension provides a substantial decrease in the field strength required to promote drop breakup because the critical *Ca* can now be reached at lower values of the electric field. The shapes of the drop containing surfactant alone, and the drop with surfactant and particles is depicted in figure 3(*a*). Instead of achieving breakup via tip-streaming from pointed ends, the drop now breaks up through the formation of two bulbous ends connected by a thin midsection. More strikingly, although the particles acquire charge at this surfactant concentration[35], the addition of particles to the drop that contains surfactant does not qualitatively change the breakup mode.

The drop containing carbon black particles stabilized by OLOA surfactant and the drop containing surfactant alone are then exposed to an electric field of $E_\infty = 5.3$ kV/cm (Supplementary movies 3, 4; ESI†). The transient shapes of the drop with and without particles are illustrated in figure 3(*b*). Unlike figure 3(*a*), however, the drops pertaining to these two systems show signs of inhomogeneity in the shape of the lobes towards the onset of breakup, as illustrated by the frame at 3.4 s. The lobes at either side of the midsection acquire a non-uniform shape, eventually achieving a non-axisymmetric, three-dimensional breakup. This transition in breakup mode of a drop of a more conducting fluid suspended in a less conducting fluid on increasing the electric field beyond the critical field for breakup was observed by Karyappa *et al.*[41]. The homogeneous breakup at lower electric fields was broadly termed as an axisymmetic shape prior to breakup (ASPB), and the inhomogeneous breakup mode at higher fields was termed non-axisymmetric shape at breakup (NASB). The onset of inhomogeneity is faster for the drop containing particles (at 2.6 s), however, similar to observations at the lower field strength, both the drops with surfactant alone, and with surfactant and particles undergo a qualitatively similar, non-axisymmetric breakup.

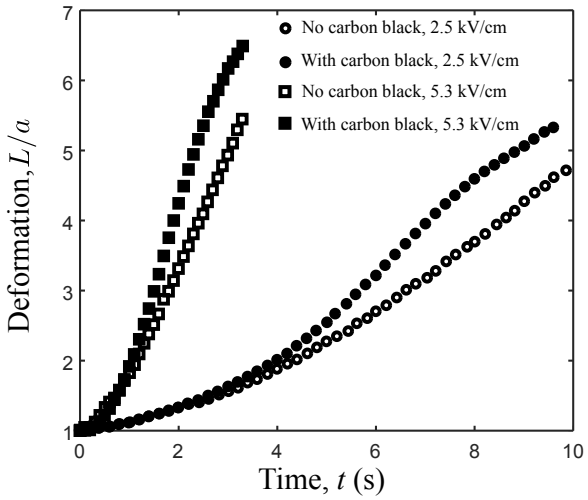

Fig. 4 Transient deformation of a squalane drop containing 0.12 wt% OLOA surfactant (open symbols), and a drop containing 3.3 g/L carbon black and 30 pph OLOA surfactant (closed symbols) subjected to an electric field of 2.5 kV/cm (circles), and 5.3 kV/cm (squares). Here, the drops are suspended in silicone oil.

The transient deformation of the drops containing surfactant,

with and without carbon black is depicted by the closed and open symbols, respectively, in figure 4. Due to the higher capillary number at 5.3 kV/cm (see table 3), the drop deformation before breakup is larger and the time scale over which the breakup occurs is shorter when compared to the experiment at the lower field. The curves that quantify the drop deformation in figure 4, and the images shown in figure 3 suggest that the development of the drop shape, the onset of drop breakup, and the actual breakup process of a drop with surfactant and carbon black is qualitatively similar to that of a drop with surfactant alone. We assert that this is due to the fact that the carbon black suspension is stable within the timescale of the experiment. The stable nature of the colloidal suspension in turn yields homogeneous drop breakup that resembles the breakup of a drop with no carbon black and an equivalent amount of surfactant. The dispersion acts only to change material properties, and the drop can be treated as homogeneous. Figure 4 shows that at early times ($t \leq 4$ s for the 2.5 kV/cm experiment, and $t \leq 2$ s for the 5.3 kV/cm experiment) the two experimental curves overlap. As time progresses, the two curves deviate from one another until the onset of drop breakup. At times $t > 5$ s and $t > 3$ s for the 2.5 kV/cm and 5.3 kV/cm experiments, respectively, the measurement for the system with carbon black and 30 pph OLOA displays a change in both slope and concavity in comparison to the system with no carbon black, finally ending with a breakup conformation that slightly exceeds the measurement for the drop with surfactant only. Although the final deformation at breakup is different at the same field strengths, the addition of particles does not significantly change the time at which breakup is observed, or the qualitative nature of breakup.

3.3 Breakup of a drop containing an unstable colloidal suspension

The field induced breakup of a drop containing 3.3 g/L carbon black with 2 pph added OLOA surfactant is examined at the same field strengths applied in the previous section. In this system, the lower concentration of added surfactant provides short-term steric stabilization of the colloidal suspension. As soon as the 2 pph sample undergoes the sonication process, the carbon black particles begin to flocculate. The aggregation time is within the timescale of the experimental measurement (minutes). The suspension forms aggregates of carbon black particles across the cell used in Electrochemical Impedance Spectroscopy. The resulting percolated network makes it difficult to determine the electrical conductivity of this system; hence a value is not reported in Table 1. The conductivity of the system is expected to exhibit a lower value than the 30 pph system, as the concentration of added surfactant is presumed to yield no electrostatic stabilization of the colloidal suspension. The transient drop shape for this system at the lower field strength of $E_\infty = 2.5$ kV/cm is depicted in the right panel of figure 5(a) (Supplementary movie 5, ESI†). As a basis for comparison, the shapes of a drop containing an equivalent amount of surfactant as the 2 pph system (0.008 wt% OLOA) and no carbon black is presented in the left panel (Supplementary movie 6, ESI†). The drop begins to exhibit a non-homogeneous shape at around $t = 3.6$ s, eventually achieving a radically different breakup mode from that of the 30 pph system illustrated in figure 3, and the drop having equivalent amount of surfactant but no particles. Here, the extremities of the drop, which are attached by a thin midsection, yield asymmetric lobes that form fingers that extend into each electrode and eventually disintegrate. This unstable, three–dimensional drop breakup mechanism likely occurs due to the formation of carbon black aggregates during the timescale of the experiment. Inhomogeneities in carbon black concentration and aggregate size within the drop arise due to the sedimentation of these colloidal clusters towards the bottom of the drop (into the page for the images presented in figure 5). We note that unlike the system described in figure 3, this non-axisymmetric drop breakup mode occurs at all applied field strengths that yield a capillary number greater than the critical capillary number Ca_c. That is, the unstable nature of the colloidal suspension always yields inhomogeneous, three-dimensional drop breakup. The experimental measurement for the drop containing an equivalent amount of surfactant as the 2 pph system and no carbon black particles displays a homogeneous, axisymmetric breakup configuration via end pinching (figure 5(a)).

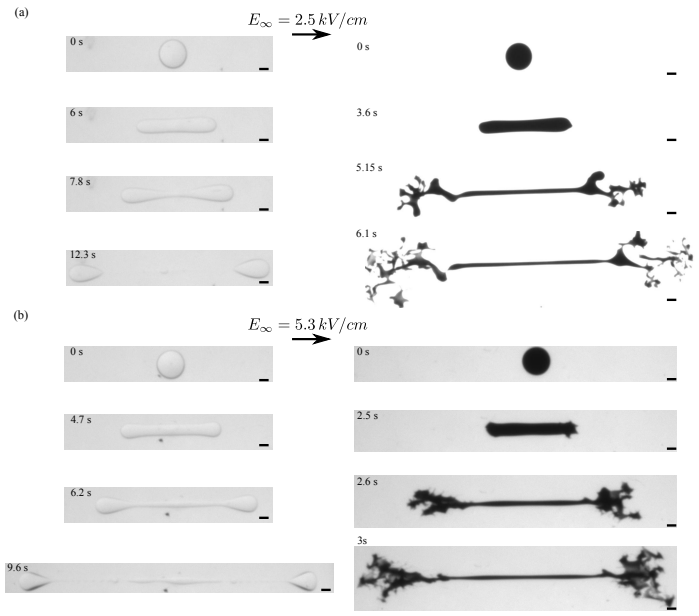

Fig. 5 Transient shapes of a drop of squalane with 0.008 wt% OLOA surfactant (left panel), and a drop of squalane with 3.3 g/L carbon black and 2 pph OLOA surfactant (right panel), subjected to an electric field of (a) 2.5 kV/cm, and (b) 5.3 kV/cm. Here, the drops are suspended in silicone oil. Scale bar: 0.5 mm

Increasing the applied field to $E_\infty = 5.3$ kV/cm yields the experimental observations depicted in figure 5(b) (Supplementary movies 7, 8; ESI†). Unlike the 30 pph systems presented in figure 3(b) for the same electric field strength, the measurement for the 2 pph system with no carbon black displays homogeneous, axisymmetric drop breakup. Although not shown in this work, further increasing the applied field beyond the value $E_\infty = 5.3$ kV/cm did not provide a qualitatively different drop breakup conforma-

tion from that illustrated in figure 5 for the system with no carbon black. Comparing figure 3(b) against figure 5(b) suggests that for the case of drops exclusively containing surfactant, the amount of the added surfactant plays a major role in determining the electric field at which the onset of inhomogeneous, three-dimensional drop breakup is achieved. Once again, the drop containing an unstable suspension yields a highly non-axisymmetric breakup, which is radically different from the breakup of the drop without particles.

The transient drop deformation for the 2 pph system at low and high fields is shown in figure 6. The closed symbols correspond to systems having carbon black and surfactant, and the open symbols represent systems containing surfactant alone. It is clear that the addition of particles at this concentration of surfactant reduces the time at which breakup is observed by almost a factor of 3. This is in stark contrast to the results obtained for the 30 pph system (figure 4), where the particles do not show a significant quantitative difference in the breakup time. Furthermore, as stated previously, the addition of carbon black does not provide an appreciable difference in the qualitative drop breakup mechanism between the 30 pph systems with and without particles. However, as presented in figure 5, this is not the case for the 2 pph systems. As the timescale for colloidal stability of the 2 pph system with carbon black becomes relevant (i.e. within the timescale of the experiment), the addition of the particles to squalane yields a radically different electric field induced drop breakup mechanism in comparison to the 30 pph system, for which the suspension was stable and the timescale for aggregation was much larger than the timescale of the experiment.

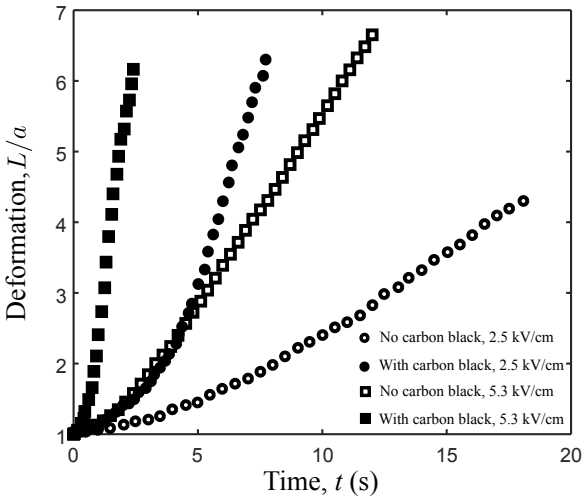

Fig. 6 Transient deformation of a squalane drop containing 0.008 wt% OLOA surfactant (open symbols), and a drop containing 3.3 g/L carbon black and 2 pph OLOA surfactant (closed symbols) subjected to an electric field of 2.5 kV/cm (circles), and 5.3 kV/cm (squares). Here, the drops are suspended in silicone oil.

4 Discussion

We examine the breakup mechanism of the squalane drop without surfactant or particles through the boundary integral computations. The electric stresses deform the drop, and the capillary stress acts to restore the equilibrium spherical shape of the drop. At the poles, the tangential component of the electric field vanishes, and the electric traction only has a normal component. This normal electric traction scales as the square of the surface charge density at the poles, $\Delta p_E = \frac{q}{2}(q+2SE_{n,i})$, where $E_{n,i}$ is the normal component of the electric field inside the drop. Figure 7 shows the evolution of the normal electric traction and the capillary stress at the poles of the squalane drop. The evolution of the surface charge density at the poles is shown in the inset. For this system, the electrohydrodynamic flow is directed to the poles of the drop. This flow convects the charge carriers towards the poles, which in turn increases the electric traction monotonically at the poles. To balance the electric traction, the capillary stress increases at the poles. Consequently, the curvature at the poles increases. Eventually, the electric stress dominates over the capillary stress, and the drop undergoes breakup by the formation of pointed ends. This mechanism has been discussed in detail[25].

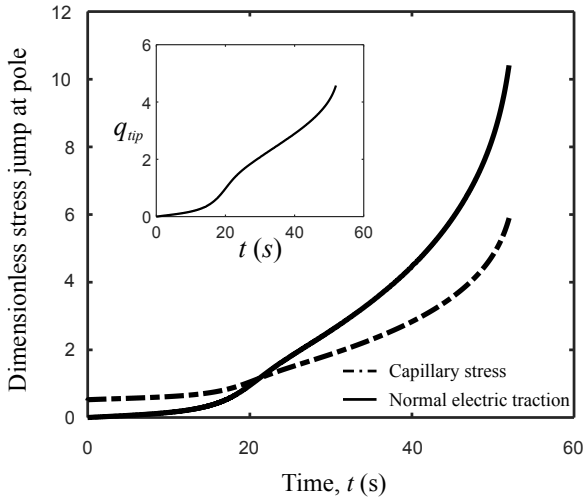

Fig. 7 Evolution of the capillary stress and normal electric traction at the pole of the drop. The material properties for this system are listed in table 1, while the relevant dimensionless groups are listed in table 2. Note that the computations assume a homogeneous drops phase.

We next aim to model the breakup of the squalane drop without particles, having a 30 pph equivalent concentration (0.12 wt%) of OLOA at 2.5 kV/cm through our boundary integral computations with insoluble surfactant. The interfacial parameters, Γ_∞ and D_s, have not been measured for a squalane-OLOA-silicone oil system, so we take values having the same order of magnitude as a surfactant at an oil-water interface. We choose $\Gamma_\infty = 2\,\mu mol/m^2$, and $D_s = 5\times10^{-10} m^2/s$, according to Alvarez *et al.*[42]. The small deformation theory predicts the interfacial tension of the squalane with 0.12 wt% OLOA in silicone oil to be slightly higher than the pure squalane-silicone oil system. This is most likely because the time scale for surfactant adsorption is slower than the time scale of drop deformation experiments, and the expected lowering of interfacial tension due to added surfactant is not captured. The interfacial tension could not be determined for the 0.008 wt% OLOA system because of the poor contrast between the drop and medium phase. For the computations, we assume that the equilibrium interfacial tension of the drop with OLOA alone is $1.4\,mN/m$,

the same as that of the drop with carbon black at 30 pph OLOA, and use the material properties and dimensionless groups corresponding to the 30 pph OLOA and carbon black system. The results of the computations for the transient drop shape are plotted against the experimental measurement in figure 8(*a*). The solid line corresponds to the result of the axisymmetric boundary integral computation with an insoluble surfactant, and the dotted line results from the computation which does not account for surfactant. Although the OLOA surfactant is soluble in squalane, we model it as an insoluble surfactant in the computations. Hence, we do not expect the computations to quantitatively capture the transient dynamics. The computation with insoluble surfactant predicts the formation of lobes at the ends of the drop, which is seen in the experiments, and the one not accounting for the surfactant becomes unstable after reaching $t = 4.8$ s, with the formation of dimples at the poles. This suggests that the transition in breakup mode from tip-streaming of a drop of pure squalane in silicone oil to end pinching of a drop of squalane with OLOA in silicone oil is due to the addition of surfactant. The electrohydrodynamic flow convects both charge carriers and surfactant molecules towards the poles of the drop, creating a non-uniform surfactant distribution at the interface, as shown in figure 8(*b*). This gives rise to Marangoni stresses, which generate a Marangoni flow to redistribute the surfactant from the poles and reestablish a uniform surfactant distribution. The Marangoni flow acts in a direction opposite to the electrohydrodynamic flow, and convects the charge carriers away from the poles. Thus, the surface charge density, and the electric traction no longer increases monotonically at the poles (figure 8(*c*)). The capillary stress is larger than the normal electric traction at the poles; eventually the drop undergoes breakup through the formation of lobes.

At a higher field of 5.3 kV/cm, this drop shows another transition to a non-axisymmetric breakup. The transition from an axisymmetric shape prior to breakup (ASPB), which occurs when the drop exhibits a uniform two-lobed shape, to a non-axisymmetric shape at breakup (NASB) was thoroughly characterized by Karyappa *et al.*[41] for conducting drops suspended in a dielectric medium (i.e. the limit of $R \to 0$). Here, at capillary numbers above the critical capillary number Ca_c for a given system, transitions from ASPB to NASB were quantified as a function of viscosity ratio, M and capillary number, Ca. For these conducting systems, a small drop viscosity, μ_i relative to the medium viscosity, μ_o ($M < 1$) yielded a transition from ASPB to NASB through the disintegration of lobes at the poles of the drop. As the viscosity ratio M was increased, the transition from ASPB to NASB shifted towards drop breakup via the formation of open jets, and finally towards breakup via the formation of jets at the poles of the drop. The breakup conformation illustrated in figure 3(*b*) resembles the drop breakup via the disintegration of lobes depicted in the work of Karyappa *et al.*[41] In particular, this form of drop breakup was labeled as "charged lobe disintegration" due to the fact that the surface charge density was maximum at the poles and neck of the multi-lobed drop. The parameters of our system at the applied electric field strength pertaining to figure 3(*b*) (i.e. $R \ll 1$, $M \ll 1$, and $Ca > Ca_c$) approach those of Karyappa *et al.*, which apply to a conducting drop suspended in a dielectric medium with a comparatively large viscosity. Thus, the drop breakup conformation depicted in figure 3(*b*) could correspond to charged lobe disintegration.

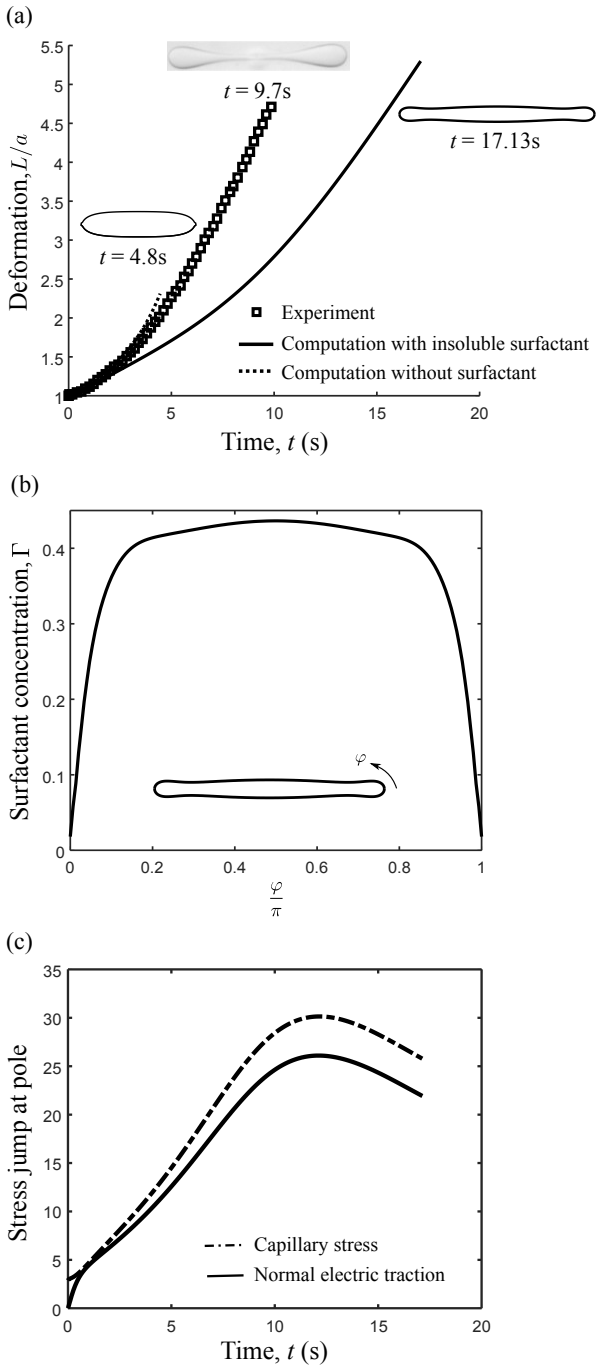

Fig. 8 (a) Experiment and computations illustrating the transient deformation of a squalane drop containing 0.12 wt% OLOA surfactant. Here the drop is suspended in silicone oil and the applied field strength is 2.5 kV/cm. (b) Distribution of surfactant concentration at the interface at $t = 17.13s$. (c) Evolution of the capillary traction and normal electric traction at the pole ($\varphi = 0$) of the drop. The material properties for this system are listed in table 1, while the relevant dimensionless groups are listed in table 2. Note that the computations assume a homogeneous drops phase.

The electric field induced breakup of the drops correspond-

ing to the 2 pph systems consisting of carbon black together with added surfactant is remindful of the Saffman-Taylor instability[43,44]. Here, a fluid displaces and fingers through a suspending medium with a comparatively large viscosity and density, and leads to patterns akin to those in the right panel of figure 5. Following the approach Karyappa *et al.*[41] applied to the breakup of conducting drops exposed to electric fields, to check whether the instability in these figures is related to the Saffman–Taylor instability, we calculate the critical wavelength above which the interface loses stability and becomes susceptible to viscous fingering, given as[43]

$$l_{\text{crit}} = 2\pi\gamma^{\frac{1}{2}} b \left[12U(\mu_o - \mu_i) + b^2 g(\rho_o - \rho_i)\right]^{-\frac{1}{2}}, \qquad (1)$$

where b represents the lobe radius, $U \sim \varepsilon_o E_\infty^2 a/\mu_o$ is a characteristic velocity scale that may be expressed in terms of the applied field by balancing the scaling for electrical stress against that for the viscous stress, g denotes the gravitational acceleration, and $\rho_{i,o}$ represents the fluid density for the drop and medium, respectively. For the field values $E_\infty = 2.5\,\text{kV/cm} - 5.3\,\text{kV/cm}$ applied in our experiments, we obtain a characteristic velocity with the range $U \sim 0.19\,\text{mm/s} - 0.87\,\text{mm/s}$. Inserting these values for the velocity scale, interfacial tension and fluid viscosities from table 1, together with the typical lobe size $b = 0.25\,\text{mm}$ measured in our experiments, and the fluid densities $\rho_i = 810\,\text{kg/m}^3$ and $\rho_o = 960\,\text{kg/m}^3$ of our system into (1) yields a critical wavelength, $l_{\text{crit}} = 0.63\,\text{mm}$. This wavelength is comparable to the lobe size, b measured in our experiments; however only the system with unstable suspension shows the inhomogeneous breakup akin to viscous fingering. Thus, the instability illustrated in the right panel of figure 5 may not be a result of the Saffman-Taylor instability, but the unstable nature of the suspension.

Carbon black particles in the 2 pph system completely sediment out of solution, yielding a clear supernatent in a time scale of minutes. The particles start forming aggregates faster than this time scale. The capillary time scale, and the flow time scale are both $\sim 0.01\,\text{s}$. Thus, the formation of aggegates will be affected by the stretching of the drop and the internal electrohydrodynamic flow. A quantitative analysis of this coupling of the flow, deformation and aggregation requires a more detailed study. To assess this phenomenon qualitatively, a drop of the 2 pph system with carbon black was aged in the cell for a prolonged amount of time before an electric field of $E_\infty = 2.5\,\text{kV/cm}$ was applied. The transient drop configuration results is that given by the closed squares in figure 9(a). Squalane is less dense than silicone oil. A time of 11 minutes was chosen before applying the field, since that is the timeframe for the squalane drop to rise from the bottom of the cell towards the middle of the two $5\,\text{cm} \times 5\,\text{cm}$ electrodes, where the field is presumed to be uniform. Keeping the drop suspended for this amount of time allows for the carbon black particles to further flocculate and form aggregates that sediment towards the bottom of the drop by the time the field is applied. The experimental measurement for the 2 pph system with and without particles, that was subjected to an electric field immediately after the drop was generated is depicted by the closed and open circles, respectively, as a basis for comparison. Note that this is the same measurement as that depicted by the circles in figure 6. Here, the drop that has been suspended for 11 minutes attains a non-spheroidal shape at a slightly earlier stage of the deformation process, as shown in figure 9(b) at $t = 3\,\text{s}$, when compared to figure 5(a). The drop proceeds to extend and achieve breakup through the formation of a continually thinning midsection with lobes at each end that eventually form fingers that extend towards the electrodes and disintegrate (figure 9(b)). This unstable drop breakup mode, which was also observed for the system corresponding to the measurement depicted by the closed circles, now occurs when the drop is relatively less extended. This is due to the extended period of time during which the drop was suspended and the colloidal suspension was allowed to destabilize under no applied field.

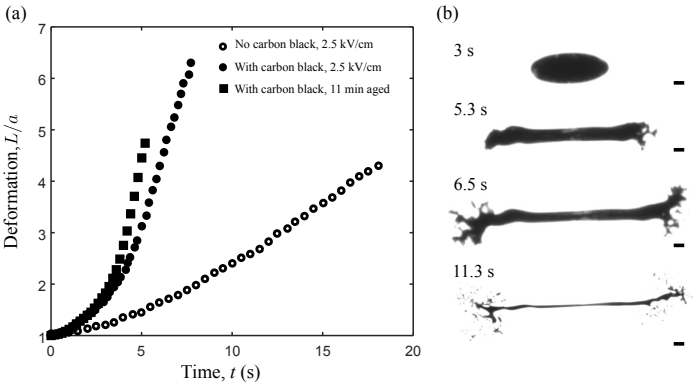

Fig. 9 (a) Transient deformation of a squalane drop containing 0.008 wt% OLOA surfactant (open circles), a drop containing 3.3 g/L carbon black and 2 pph OLOA surfactant subjected to an electric field of 2.5 kV/cm instantaneously (closed circles), and a drop containing 3.3 g/L carbon black and 2 pph OLOA surfactant subjected to an electric field of 2.5 kV/cm, 11 minutes after the drop is generated (closed squares). (b) Transient drop shapes of a squalane drop containing 3.3 g/L carbon black and 2 pph OLOA subjected to an electric field of 2.5 kV/cm, 11 minutes after the drop is generated. Here, the drops are suspended in silicone oil. Scale bar: 0.5 mm.

5 Conclusions

This work demonstrates the impact of colloidal stability on breakup of drops under an electric field. Stability on the time scale of deformation leads to rich and unexplored breakup phenomena. We have quantified the breakup of a low conductivity squalane drop containing a suspension of carbon black particles and varying amounts of polyisobutylene succinimide (OLOA) surfactant. For a fixed concentration of 3.3 g/L carbon black and a mass fraction of 30 parts OLOA per 100 parts carbon black (pph OLOA), an applied field of $E_\infty = 2.5\,\text{kV/cm}$ yielded homogeneous drop breakup via the pinch-off of bulbous ends. When the electric field was increased to $E_\infty = 5.3\,\text{kV/cm}$, the drop achieved inhomogeneous, three-dimenisonal breakup. This drop breakup mechanism was labeled as "charged lobe disintegration" by Karyappa *et al.*[41] The breakup of a drop containing both carbon black particles and 30 pph added OLOA did not display any appreciable qualitative differences from the breakup of a drop containing an equivalent amount of surfactant and no carbon black, regardless

of the applied electric field strength. This was due to the stability of the dilute colloidal suspension on a timescale much longer than that of the experiment (months). Here, the stable nature of the suspended carbon black particles did not yield any inhomogeneities in the electric field induced breakup of the squalane drop.

Lower concentrations of surfactant (2 pph OLOA) yielded inhomogeneous drop breakup at applied fields that matched or exceeded the critical electric field strength, in which the lobes at each end of the drop formed fingers that extended towards the electrodes and eventually disintegrated. For this system, the lower amount of surfactant provided short-term stability of the carbon black particles. The colloidal suspension of carbon black began to flocculate as soon as the drop was generated and the aggregates sedimented towards the bottom of the drop within the timescale of the experiment (minutes). Here, the unstable nature of the suspension yielded inhomogeneous, three-dimensional drop breakup at all applied fields in our experiments, which drops containing the same amount of added OLOA and no carbon black did not exhibit. Extending the aggregation time of the suspension before the uniform field was applied yielded the same qualitative drop breakup mode at lower aspect ratios.

The experimental procedure presented in this work may be implemented as means to rapidly deduce the colloidal stability of a suspension. A determination of the suspension stability would consist of slowly increasing the applied electric field across a suspended suspension-loaded drop until the critical field strength is reached. Based on the results presented in this work, a colloidal suspension that is stable over the timescale of the experiment would yield homogeneous, axisymmetric drop breakup. Further increasing the applied field, such that the capillary number surpasses the critical electric capillary number Ca_c, would yield a non-axisymmetric shape during breakup [41]. If the colloidal suspension is unstable over experimental timescales, the critical electric field strength would provide an inhomogeneous, three-dimensional drop breakup conformation. This form of breakup does not qualitatively vary when the field is increased such that $Ca > Ca_c$.

In addition to serving as a rapid determination of the colloidal stability of a suspension within a liquid drop, our findings could serve as means to achieve a desired electric field induced drop breakup mechanism. By tuning the electrical properties and viscosity of the two fluids, as well as the degree of colloidal stability of the suspension within the drop, and the applied field strength, one may ensure that a particular drop breakup mode is achieved (e.g. axisymmetric drop breakup via the pinch-off of bulbous ends), or that drop breakup is completely circumvented for a given experimental system. This is relevant for applications such as inkjet printing, in which the stability of a colloidal suspension within a drop is desired under the action of an electric field to prevent inhomogenous, three-dimensional breakup of the ink drops [45]; or electroemulsification where colloidal instability can promote drop breakup at lower field strengths, reducing the power requirement for emulsification. The present work highlights the importance of colloidal stability on the breakup of suspension-loaded drops under electric fields

Acknowledgments

We are grateful for support by the National Science Foundation through grant number CBET–1066853, and partial support by the John E. Swearingen Graduate Fellowship to RS.

References

1 B.-J. de Gans, P. C. Duineveld and U. S. Schubert, *Advanced materials*, 2004, **16**, 203–213.
2 J.-U. Park, M. Hardy, S. J. Kang, K. Barton, K. Adair, D. kishore Mukhopadhyay, C. Y. Lee, M. S. Strano, A. G. Alleyne, J. G. Georgiadis *et al.*, *Nature materials*, 2007, **6**, 782.
3 M. Singh, H. M. Haverinen, P. Dhagat and G. E. Jabbour, *Advanced materials*, 2010, **22**, 673–685.
4 T. Scott and W. Sisson, *Separation Science and technology*, 1988, **23**, 1541–1550.
5 T. C. Scott, D. W. DePaoli and W. G. Sisson, *Industrial & engineering chemistry research*, 1994, **33**, 1237–1244.
6 R. B. Karyappa, A. V. Naik and R. M. Thaokar, *Langmuir*, 2015, **32**, 46–54.
7 J. B. Fenn, M. Mann, C. K. Meng, S. F. Wong and C. M. Whitehouse, *Science*, 1989, **246**, 64–71.
8 R. L. Grimm and J. L. Beauchamp, *The Journal of Physical Chemistry B*, 2005, **109**, 8244–8250.
9 B. Derby, *Journal of Materials Chemistry*, 2008, **18**, 5717–5721.
10 P. Dommersnes, Z. Rozynek, A. Mikkelsen, R. Castberg, K. Kjerstad, K. Hersvik and J. O. Fossum, *Nat. Commun.*, 2013, **4**, year.
11 M. Ouriemi and P. M. Vlahovska, *J. Fluid Mech.*, 2014, **751**, 106–120.
12 Z. Rozynek, P. Dommersnes, A. Mikkelsen, L. Michels and J. Fossum, *The European Physical Journal Special Topics*, 2014, **223**, 1859–1867.
13 Z. Rozynek, A. Mikkelsen, P. Dommersnes and J. O. Fossum, *Nat. Commun.*, 2014, **5**, year.
14 G. Taylor, *Proceedings of the Royal Society of London. Series A. Mathematical and Physical Sciences*, 1964, **280**, 383–397.
15 G. I. Taylor, *Proc. R. Soc. London, Ser. A*, 1966, **291**, 159–166.
16 J. Zeleny, *Physical review*, 1917, **10**, 1.
17 J. D. Sherwood, *J. Fluid Mech.*, 1988, **188**, 133–146.
18 J. Q. Feng and T. C. Scott, *J. Fluid Mech.*, 1996, **311**, 289–326.
19 J. Q. Feng, *Proc. R. Soc. London, Ser. A*, 1999, **455**, 2245–2269.
20 E. Lac and G. M. Homsy, *J. Fluid Mech.*, 2007, **590**, 239–264.
21 R. T. Collins, J. J. Jones, M. T. Harris and O. A. Basaran, *Nature Physics*, 2008, **4**, 149.
22 R. T. Collins, K. Sambath, M. T. Harris and O. A. Basaran, *Proc. Natl. Acad. Sci. USA*, 2013, **110**, 4905–4910.
23 J. A. Lanauze, L. M. Walker and A. S. Khair, *J. Fluid Mech.*, 2015, **774**, 245–266.
24 D. Das and D. Saintillan, *Journal of Fluid Mechanics*, 2017, **810**, 225–253.
25 R. Sengupta, L. M. Walker and A. S. Khair, *Journal of Fluid*

Mechanics, 2017, **833**, 29–53.
26 S. Torza, R. G. Cox and S. G. Mason, *Philos. Trans. R. Soc. London, Ser. A*, 1971, **269**, 295–319.
27 O. Vizika and D. A. Saville, *J. Fluid Mech.*, 1992, **239**, 1–21.
28 J.-W. Ha and S.-M. Yang, *J. Fluid Mech.*, 2000, **405**, 131–156.
29 P. F. Salipante and P. M. Vlahovska, *Phys. Fluids*, 2010, **22**, 112110.
30 J.-W. Ha and S.-M. Yang, *Journal of colloid and interface science*, 1998, **206**, 195–204.
31 J. S. Raut, S. Akella, A. Singh and V. M. Naik, *Langmuir*, 2009, **25**, 4829–4834.
32 P. Calvert, *Chemistry of materials*, 2001, **13**, 3299–3305.
33 R. J. Pugh, T. Matsunaga and F. M. Fowkes, *Colloids and Surfaces*, 1983, **7**, 183–207.
34 R. J. Pugh and F. M. Fowkes, *Colloids and surfaces*, 1984, **9**, 33–46.
35 B. J. Bleier, B. A. Yezer, B. J. Freireich, S. L. Anna and L. M. Walker, *Journal of colloid and interface science*, 2017, **493**, 265–274.
36 B. A. Yezer, A. S. Khair, P. J. Sides and D. C. Prieve, *J. Colloid Interface Sci.*, 2014, **449**, 2–12.
37 J. A. Lanauze, L. M. Walker and A. S. Khair, *Phys. Fluids*, 2013, **25**, 112101.
38 J. R. Melcher and G. I. Taylor, *Annu. Rev. Fluid Mech.*, 1969, **1**, 111–146.
39 D. A. Saville, *Annu. Rev. Fluid Mech.*, 1997, **29**, 27–64.
40 H. Stone, *Physics of Fluids A: Fluid Dynamics*, 1990, **2**, 111–112.
41 R. B. Karyappa, S. D. Deshmukh and R. M. Thaokar, *Journal of Fluid Mechanics*, 2014, **754**, 550–589.
42 N. J. Alvarez, W. Lee, L. M. Walker and S. L. Anna, *Journal of colloid and interface science*, 2011, **355**, 231–236.
43 P. G. Saffman and G. Taylor, Proceedings of the Royal Society of London A: Mathematical, Physical and Engineering Sciences, 1958, pp. 312–329.
44 G. M. Homsy, *Annual review of fluid mechanics*, 1987, **19**, 271–311.
45 D. Kang, M. Lee, H. Y. Kim, S. James and S. Yoon, *Journal of Aerosol Science*, 2011, **42**, 621–630.

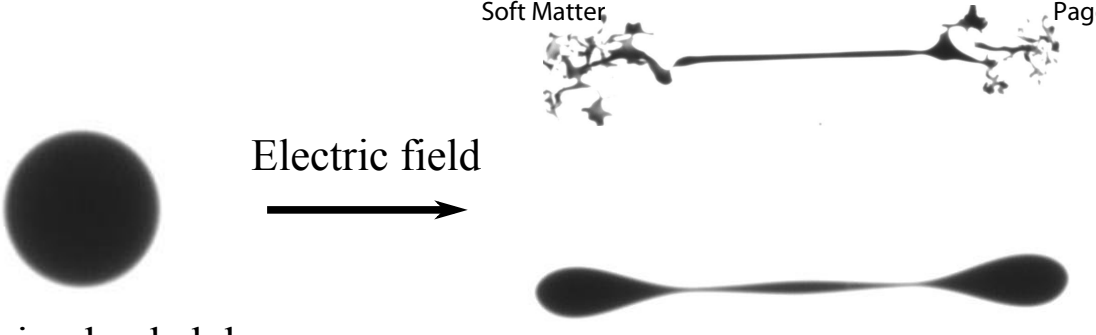
Electric field
Suspension stability
Suspension loaded drop